## Research

# Radiation attenuation effectiveness of the inverse freezing fluid - a new shielding material for gamma radiation

Reshma Karunakaran<sup>1</sup> · Rajagopal Shanmugasundaram<sup>1,2</sup>

Received: 5 March 2025 / Accepted: 21 May 2025

Published online: 13 August 2025 © The Author(s) 2025 OPEN

## **Abstract**

The inverse freezing fluids are the new field of science, in which the synthesised fluid mixtures freezes at high temperature and liquifies at lower temperature. Recently we observed such a new thermal and thermal-mechanical metamaterial behaviour from the liquid mixtures of citric acid and ethanolamine solution under different conditions. This new science is still in the basic research stage with no applications so far developed. This is the first paper which gives a detailed description about the application of such inverse freezing fluids. Here we have opted to study the gamma radiation shielding of the synthesised inverse freezing fluids (IFF) namely, pure IFF and metals such as, vanadium and molybdenum doped IFF samples. From the data reported and analysis in this manuscript, it is evident that different liquids mixtures, especially, IFF's can be used for gamma radiation shielding with varying temperature. We found better shielding parameters while taking IFF's at higher temperature. The effect of temperature has influenced the radiation absorption and transmittance through the samples. Comparison plots were given for better understanding with which the molybdenum doped sample shows better shielding than the other two samples. In case of the Co-60 source the absorption factor is 0.3418, LAC is 1.1396 cm<sup>-1</sup> and MFP was 0.8774 cm<sup>-1</sup> for molybdenum doped samples which are evidently more compared to the vanadium doped samples. To the best of our knowledge this is the first comprehensive study exploring the temperature dependent gamma attenuation properties of the soft matter which is initially in the liquid form. Fundamental discovery of such IFF's are promising research materials, in the context of emerging liquid phase systems for the radiation shielding applications.

## Highlights

- Exploring first ever novel liquid-based (IFF) material for temperature influenced gamma radiation shielding.
- Synthesis, studies and efficiency of metal doped fluid mixtures for shielding applications.
- Investigation of better shielding of molybdenum doped IFF.

**Keywords** Inverse freezing fluids · Liquid shielding · Gamma radiation · Metal doped fluids · Temperature variation · Refractive index · Absorption · Linear attenuation coefficient

Rajagopal Shanmugasundaram, raja2001s@gmail.com; s.rajagopal@psgcas.ac.in | <sup>1</sup>Department of Physics and Electronics, School of Sciences, JAIN (Deemed to be) University, #34, 1st Cross, JC Road, Near Ravindra Kalakshetra, Bangalore 560027, India. <sup>2</sup>Department of Physics, PSG College of Arts & Science, Coimbatore 641014, India.



**Discover Applied Sciences** 





## 1 Introduction

Given that radioactive materials are increasingly being used in research, agriculture, medicine, and power generation, radiation protective measures and the management of radioactive and nuclear waste have become global concerns. [1]. The risks that radioactive materials bring to humans, animals, and the environment cannot be overstated. Liquid nuclear waste is the most difficult type of radioactive waste to manage. Attenuating the high penetration of gamma radiation from liquid materials is extremely challenging. Therefore, the adoption of tailored liquid phase materials with excellent radiation shielding capabilities can lead to effective gamma radiation shielding with high linear attenuation coefficients and radioactive waste management [2, 3]. Thermal evaporation [4], chemical precipitation [5], ion exchange [6], and other techniques [7] are used in the treatment and disposal of liquid phase nuclear waste [8].

We need alternate materials for radiation shielding because of the inherent drawbacks of the well-known radiation shielding material "lead (Pb)" [9], which include toxicity (lead poisoning), corrosion, and high liquid permeability in the case of red mud. Although polymer matrixes have been employed for radiation shielding in certain situations [6–8], it should be highlighted that these materials are solids and are difficult to get rid of. Some of the polymer-based materials were also been used as shielding materials [13–17]. In contrast to lead, metals like tungsten, gadolinium, dysprosium, etc., that were infused into glasses were thought to be non-toxic and benign to the environment [18]. Some other well-established gamma radiation shielding materials are studied with different methods [19–23]. Further high temperature radiation studies were also done using cementitious composites containing nano-Ba<sub>2</sub>O<sub>3</sub> [24]. Other nano-polymer mixture composites based shielding materials were also investigated [25]. We need an alternative radiation shielding materials in liquid phase. Furthermore, different materials can be employed to shield other radiations like alpha, beta, neutron [26–32] etc.

Inverse freezing fluids are the new kind of thermal metamaterials, which exhibit a reversible phase transformation while increasing and decreasing temperature. These liquid phase thermal metamaterial mixtures freezes at higher temperature and melts at lower temperature [33]. These kind of IFF solutions are basically sustainable and remains in its phase in closed environment thus, giving long term stability, easy to store and bio degradable. In this paper, we are reporting for the first time, a set of fluid mixtures doped with metals such as vanadium and molybdenum, were studied for radiation shielding properties. This manuscript addresses an original and new research area for the first time, using inverse freezing fluids (IFFs) doped with metals such as vanadium and molybdenum, potentially flexible, liquid-phase materials to demonstrate the gamma radiation shielding properties.

## 1.1 Materials and methods

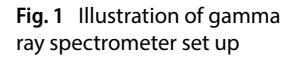
## 1.2 Materials

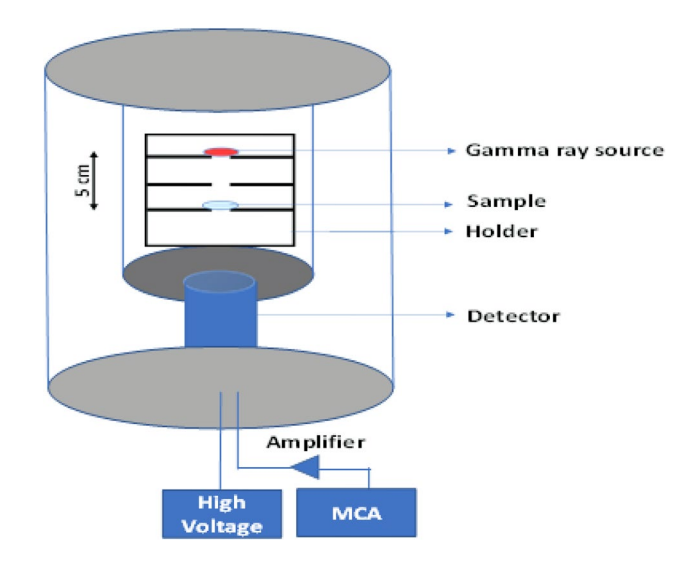
In this current study, the raw materials such as, citric acid amorphous, monoethanolamine, vanadium pentoxide, molybdenum trioxide, double distilled water were procured from SD Fine Chemicals Ltd (99.99% purity) and the same were used for the experiments without any further purification. The gamma radiation sources such from <sup>137</sup>Cs (661.6 keV), <sup>60</sup>Co (1173.2 keV), <sup>22</sup>Na (1275 keV) and <sup>133</sup>Ba (356 keV) procured from Bhaba Atomic Research Centre (BARC, Trombay).

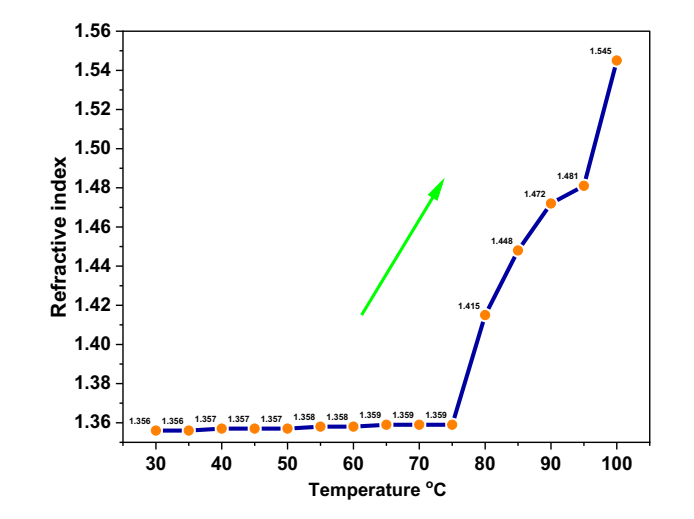
## 1.3 Synthesis method

The pure sample is prepared by mixing 1gm of amorphous citric acid in 20 ml of double distilled water followed by slow addition 5 ml of monoethanolamine. Under continuous stirring at 50 rpm, this mixture becomes viscous IFF sample with pH = 13 at ambient temperature and pressure. This sample is named as pure IFF sample and was subjected to different temperatures. This pure IFF sample's physical properties were observed by increasing its temperature for every 15 °C staring from 30 °C till 90 °C. Similarly, for doped IFF samples, 0.5 gm of vanadium pentoxide was added to the final mixture of the pure IFF sample and subjected to different temperatures as mentioned above. The observed pH of this solution was 8 and the solution was left for stirring at 50 rpm for 30 min at ambient temperature and pressure. Same procedure was followed for molybdenum trioxide doped IFF samples. The pH observed was 9 and the solution was left for stirring at 50 rpm for 30 min at ambient temperature and pressure. Five set of data points were observed by varying









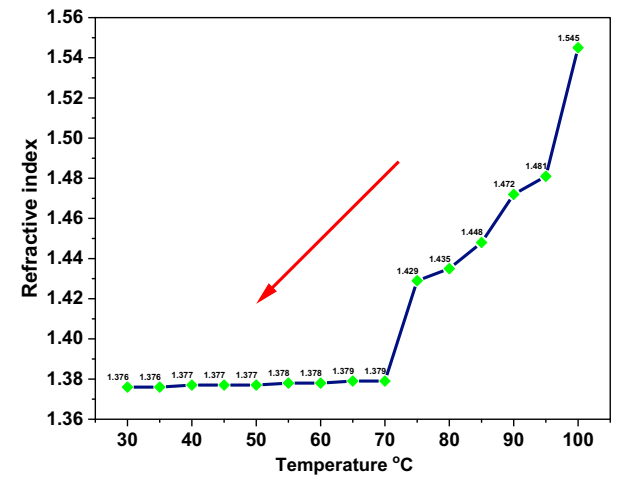
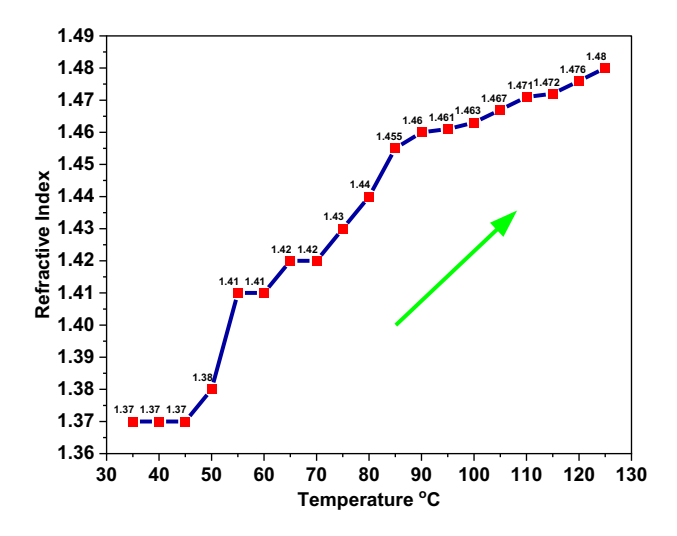


Fig. 2 Refractive indices of pure sample for increasing and decreasing temperatures



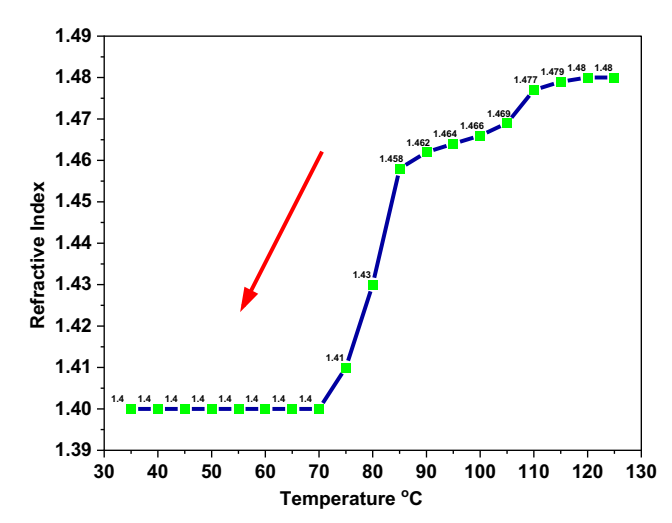


Fig. 3 Refractive indices of vanadium doped sample for increasing and decreasing temperatures



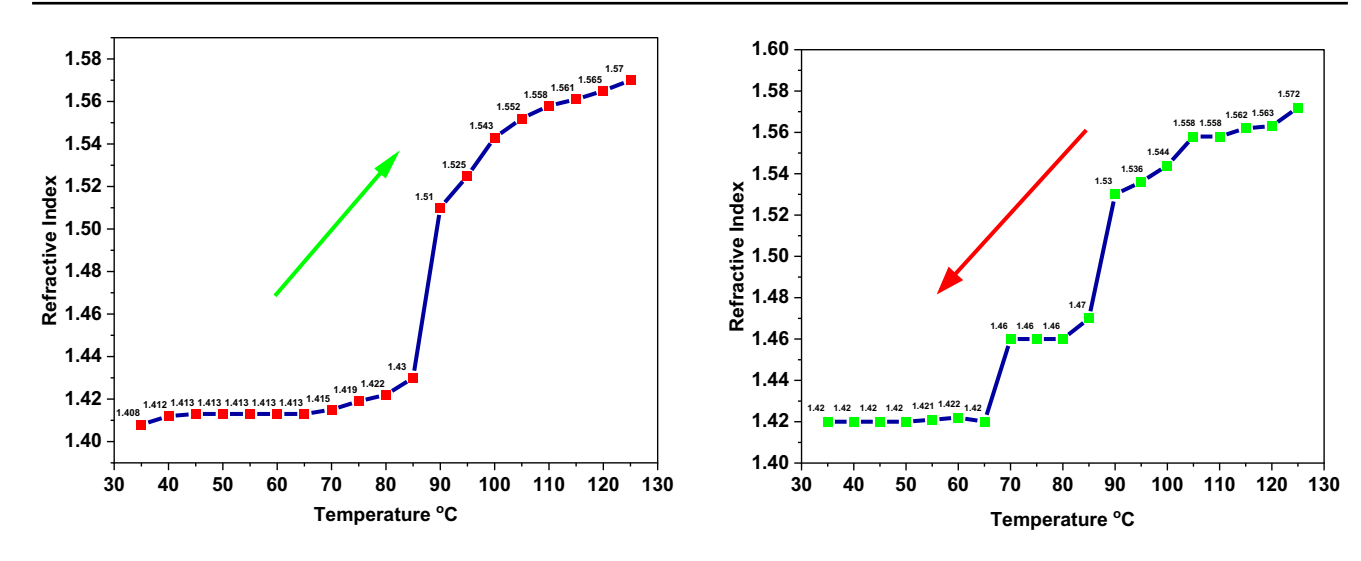


Fig. 4 Refractive indices of molybdenum doped sample for increasing and decreasing temperatures

**Table 1** Phase transition points of the fluids

Sample	Phase transition point °C			
	While increasing	While decreas- ing		
Pure IFF	75	75		
V doped IFF	45	85		
Mo doped IFF	85	92		

the temperature range from 30 to 90 °C by 15 oC interval for each precursor fluid mixture. Further, the synthesised IFF fluid samples were subjected to analyse the gamma ray shielding properties against the sources  $^{137}$ Cs (661.6 keV),  $^{60}$ Co (1173.2 keV),  $^{22}$ Na (1275 keV) and  $^{133}$ Ba (356 keV).

# 2 Experiment and characterization

The straightforward method for the identification of inverse freezing fluids is primarily determined through their refractive indices at varying temperatures. To confirm the inverse freezing phenomenon, optical characterization of the fluid mixtures was performed using an Abbe refractometer, a traditional method for measuring refractive index. Gamma ray absorption studies were conducted using four different sources: <sup>137</sup>Cs (661.6 keV), <sup>60</sup>Co (1173.2 keV), <sup>22</sup>Na (1275 keV) and <sup>133</sup>Ba (356 keV). The shielding performance was assessed by comparing different sample sets with a gamma ray scintillation spectrometer NaI(Tl) (Modular Minim Based) [TYPE: GR 611 M]. The experiments were conducted without additional reflecting or shielding materials.

For each measurement, the count rate was recorded over a 300-s interval, and three trials were performed to ensure accuracy, with the average results reported. There were not much variations in the measurements even after repeating for several thermal cycles of the prepared samples. The experimental setup, as illustrated in Fig. 1, included a gamma ray source holder for placing the radiation source at 5 cm, a plastic sample holder (which does not affect gamma ray transmission) to contain the liquid sample (with a thickness of 3 mm), the detector, and the necessary amplifiers.

The samples were irradiated with gamma photons emitted from sources including  $^{137}$ Cs (661.6 keV),  $^{60}$ Co (1173.2 keV),  $^{22}$ Na (1275 keV) and  $^{133}$ Ba (356 keV) which were procured from the Bhabha Atomic Research Centre (BARC, Trombay). The analysis involved measuring gamma radiation spectra with a point source to minimize statistical errors [34–36]. Background counts ( $I_0$ ) were recorded before exposing the samples. The transmitted spectra were then measured over a 300-s interval to ensure accuracy, with the gamma-ray scintillation detector set to 700 V. Three trials were conducted for each



sample, and the average count was used for analysis. Upon introducing the sample, intensity counts (III) were measured. The thickness of the liquid sample was directly proportional to the thickness of the sample holder, which was 3 mm.

## 3 Results and discussions

# 3.1 Optical properties

#### 3.1.1 Refractive index studies

The refractive index of the synthesized samples was analysed using an Abbe refractometer, a traditional method that confirms the inverse freezing phenomenon of the fluids. Initially, the refractive indices of plain citric acid solution and ethanolamine were measured at 1.337 [37] and 1.436 [38], respectively, at room temperature. As the temperature increases, these fluids gain viscosity and density, leading to a corresponding rise in their refractive indices, as density and refractive index are proportional.

Figure 2 illustrates the refractive indices of the pure sample at both increasing and decreasing temperatures. Starting at a refractive index of 1.356 at 30 °C, the pure sample's refractive index increases proportionally with temperature. Beyond 75 °C, the refractive index rises to 1.415, reaching up to 1.545 at temperatures above 90 °C. Upon cooling, the refractive index initially at 1.545 decreases to 1.375 at 70 °C and stabilizes around this value down to 30 °C. This behaviour confirms that the pure sample exhibits inverse freezing characteristics, solidifying at high temperatures and melting at low temperatures. Following doping with vanadium and molybdenum [39], the samples were subjected to optical analysis. Similar to the pure sample, these doped samples also demonstrated the inverse freezing phenomenon, as shown in Figs. 3 and 4.

**Table 2** Shielding properties of pure sample for Cs-137

Tempera- ture °C	l value	Transmission factor (I/Io)	Absorption	LAC μ (cm <sup>-1</sup> )	HVL (cm)	TVL (cm)	MFP (cm <sup>-1</sup> )
30	2514	0.9755	0.01074	0.0358	19.3410	64.2469	27.9091
45	2457	0.9534	0.0207	0.0690	10.0389	33.3473	14.4862
60	2286	0.8870	0.0520	0.1734	3.99514	13.2710	5.7649
75	2097	0.8137	0.0895	0.2983	2.32249	7.7148	3.3513
90	1896	0.7357	0.1332	0.4442	1.55991	5.1817	2.2509

**Table 3** Shielding properties of vanadium doped sample for Cs-137

Tempera- ture °C	l value	Transmission factor (I/Io)	Absorption	LAC μ (cm-1)	HVL (cm)	TVL (cm)	MFP (cm <sup>-1</sup> )
30	2434	0.9445	0.0247	0.0826	8.3851	27.8536	12.0997
45	2398	0.9305	0.0312	0.1042	6.6495	22.0884	9.5953
60	2237	0.8680	0.0614	0.2048	3.3833	11.2386	4.8821
75	2018	0.7830	0.1061	0.3539	1.9577	6.5032	2.8250
90	1806	0.7008	0.1543	0.5146	1.3465	4.4728	1.9430

**Table 4** Shielding properties of molybdenum doped sample for Cs-137

Tempera- ture °C	l value	Transmission factor (I/Io)	Absorption	LAC μ (cm <sup>-1</sup> )	HVL (cm)	TVL (cm)	MFP (cm <sup>-1</sup> )
30	2417	0.9379	0.0278	0.0927	7.4682	24.8080	10.7767
45	2294	0.8901	0.0505	0.1684	4.1151	13.6695	5.9381
60	2156	0.8366	0.0774	0.2582	2.6837	8.9149	3.8726
75	2009	0.7795	0.1081	0.3604	1.9226	6.3864	2.7743
90	1785	0.6926	0.1594	0.5315	1.3036	4.3304	1.8811



Table 5	Shielding properties
of pure	sample for Na-22

Tempera- ture °C	l value	Transmission factor (I/Io)	Absorption	LAC μ (cm <sup>-1</sup> )	HVL (cm)	TVL (cm)	MFP (cm <sup>-1</sup> )
30	1289	0.9839	0.0070	0.0233	29.6222	98.3987	42.7449
45	1210	0.9236	0.0344	0.1149	6.0285	20.0255	8.6992
60	1186	0.9053	0.0431	0.1439	4.8139	15.991	6.9465
75	1078	0.8229	0.0846	0.2821	2.4559	8.158	3.5438
90	995	0.7595	0.1194	0.3981	1.7405	5.7815	2.5115

**Table 6** Shielding properties of vanadium doped sample for Na-22

Tempera- ture °C	l value	Transmission factor (I/Io)	Absorption	LAC μ (cm <sup>-1</sup> )	HVL (cm)	TVL (cm)	MFP (cm <sup>-1</sup> )
30	1209	0.9229	0.0348	0.1161	5.9664	19.8192	8.6095
45	1190	0.9083	0.0417	0.1390	4.9827	16.5514	7.1900
60	1096	0.8366	0.0774	0.2582	2.6839	8.9154	3.8729
75	978	0.7465	0.1269	0.4231	1.6378	5.4406	2.3634
90	895	0.6832	0.1654	0.5514	1.2565	4.1741	1.8132

**Table 7** Shielding properties of molybdenum doped sample for Na-22

Tempera- ture °C	I value	Transmission factor (I/Io)	Absorption	LAC μ (cm <sup>-1</sup> )	HVL (cm)	TVL (cm)	MFP (cm <sup>-1</sup> )
30	1202	0.9175	0.0373	0.1245	5.5637	18.4816	8.02851
45	1110	0.8473	0.0719	0.2398	2.8895	9.5985	4.1696
60	1006	0.7679	0.1146	0.3822	1.8129	6.0223	2.6161
75	975	0.7442	0.1282	0.4275	1.6208	5.3840	2.3388
90	887	0.6770	0.1693	0.5644	1.2276	4.0780	1.7715

**Table 8** Shielding properties of pure sample for Co-60

Tempera- ture °C	l value	Transmission factor (I/Io)	Absorption	LAC μ (cm <sup>-1</sup> )	HVL (cm)	TVL (cm)	MFP (cm <sup>-1</sup> )
30	1573	0.9609	0.0173	0.0577	12.0034	39.8730	17.3210
45	1478	0.9028	0.0443	0.1479	4.6851	15.5630	6.7606
60	1275	0.7788	0.1085	0.3617	1.9154	6.3627	2.7639
75	1167	0.7128	0.1469	0.4899	1.4144	4.6986	2.0411
90	1087	0.6640	0.1778	0.5927	1.1691	3.8837	1.6871

**Table 9** Shielding properties of vanadium doped sample for Co-60

Tempera- ture °C	l value	Transmission factor (I/Io)	Absorptio	LAC μ (cm <sup>-1</sup> )	HVL (cm)	TVL (cm)	MFP (cm <sup>-1</sup> )
30	1498	0.9150	0.0385	0.1284	5.3948	17.9205	7.7847
45	1318	0.8051	0.0941	0.3137	2.2085	7.3364	3.1869
60	1185	0.7238	0.1403	0.4677	1.4815	4.9212	2.1378
75	967	0.5907	0.2286	0.7620	0.9093	3.0207	1.3122
90	885	0.5406	0.2671	0.8903	0.7783	2.5854	1.1231

Subsequent to this refractive index analysis, the phase transition points of the fluids were identified and presented in Table 1. From the table it is evident that the phase transition temperatures of the samples were low while increasing the temperature and it's notably high while decreasing the temperature. Thus, it could be interpreted that addition of metals have tuned the optical properties of the samples.



**Table 10** Shielding properties of molybdenum doped sample for Co-60

Tempera- ture °C	l value	Transmission factor (I/Io)	Absorption	LAC μ (cm <sup>-1</sup> )	HVL (cm)	TVL (cm)	MFP (cm <sup>-1</sup> )
30	1473	0.8998	0.0458	0.1528	4.5347	15.0634	6.5436
45	1278	0.7806	0.1075	0.3583	1.9336	6.4231	2.7902
60	1105	0.6750	0.1706	0.5689	1.2180	4.0460	1.7576
75	958	0.5852	0.2326	0.7756	0.8934	2.9679	1.2893
90	745	0.4551	0.3418	1.1396	0.6080	2.0199	0.8774

**Table 11** Shielding properties of pure sample for Ba-133

Tempera- ture °C	l value	Transmission factor (I/Io)	Absorption	LAC μ (cm <sup>-1</sup> )	HVL (cm)	TVL (cm)	MFP (cm <sup>-1</sup> )
30	11,643	0.9755	0.0107	0.0358	19.3260	64.1969	27.8874
45	11,373	0.9529	0.0209	0.0698	9.9248	32.9683	14.3215
60	11,056	0.9263	0.0332	0.1107	6.2574	20.7859	9.02951
75	10,046	0.8417	0.0748	0.2494	2.7783	9.2290	4.00912
90	8985	0.7528	0.1233	0.4110	1.6860	5.6007	2.43300

**Table 12** Shielding properties of vanadium doped sample for Ba-133

Tempera- ture °C	I value	Transmission factor (I/Io)	Absorption	LAC μ (cm <sup>-1</sup> )	HVL (cm)	TVL (cm)	MFP (cm <sup>-1</sup> )
30	11,576	0.9699	0.0132	0.0442	15.6741	52.0661	22.6177
45	11,276	0.9447	0.0246	0.0822	8.4281	27.9965	12.1618
60	10,083	0.8448	0.0732	0.2441	2.8388	9.4302	4.0965
75	9564	0.8013	0.0961	0.3206	2.1615	7.1800	3.1190
90	7756	0.6498	0.1871	0.6239	1.1106	3.6894	1.6026

**Table 13** Shielding properties of molybdenum doped sample for Ba-133

Tempera- ture °C	I value	Transmission factor (I/Io)	Absorption	LAC μ (cm <sup>-1</sup> )	HVL (cm)	TVL (cm)	MFP (cm <sup>-1</sup> )
30	11,434	0.9580	0.0186	0.0620	11.1628	37.0807	16.1080
45	11,173	0.9361	0.0286	0.0955	7.2558	24.1025	10.4702
60	9566	0.8015	0.0960	0.3203	2.1635	7.1868	3.1220
75	8237	0.6901	0.1610	0.5368	1.2908	4.2880	1.8627
90	7981	0.6687	0.1747	0.5825	1.1895	3.9515	1.7165

## 3.2 Radiation shielding property

Radiation shielding materials are typically composed of high atomic number (Z) elements or compounds, which enhance their capacity to attenuate radiation. But these fluid samples are designed as suspensions or solutions with low atomic number elements to leverage the dynamic properties of liquids to provide adaptive and uniform shielding coverage. Unlike traditional solid shields, liquid shields can conform to various geometries, making them particularly suitable for complex or irregularly shaped environments. The practical implementation of liquid radiation shielding involves careful consideration of factors such as viscosity, chemical stability, and compatibility with existing systems.

The linear attenuation coefficient (LAC) is a crucial parameter for assessing gamma radiation shielding effectiveness [40]. While previous studies predominantly focused on variations in density and photon energy for glass materials [41, 42], this paper introduces a novel approach by examining radiation shielding with liquid samples at varying temperatures. Our findings reveal a significant increase in the LAC with rising temperature, aligning with Beer-Lambert's law. Among



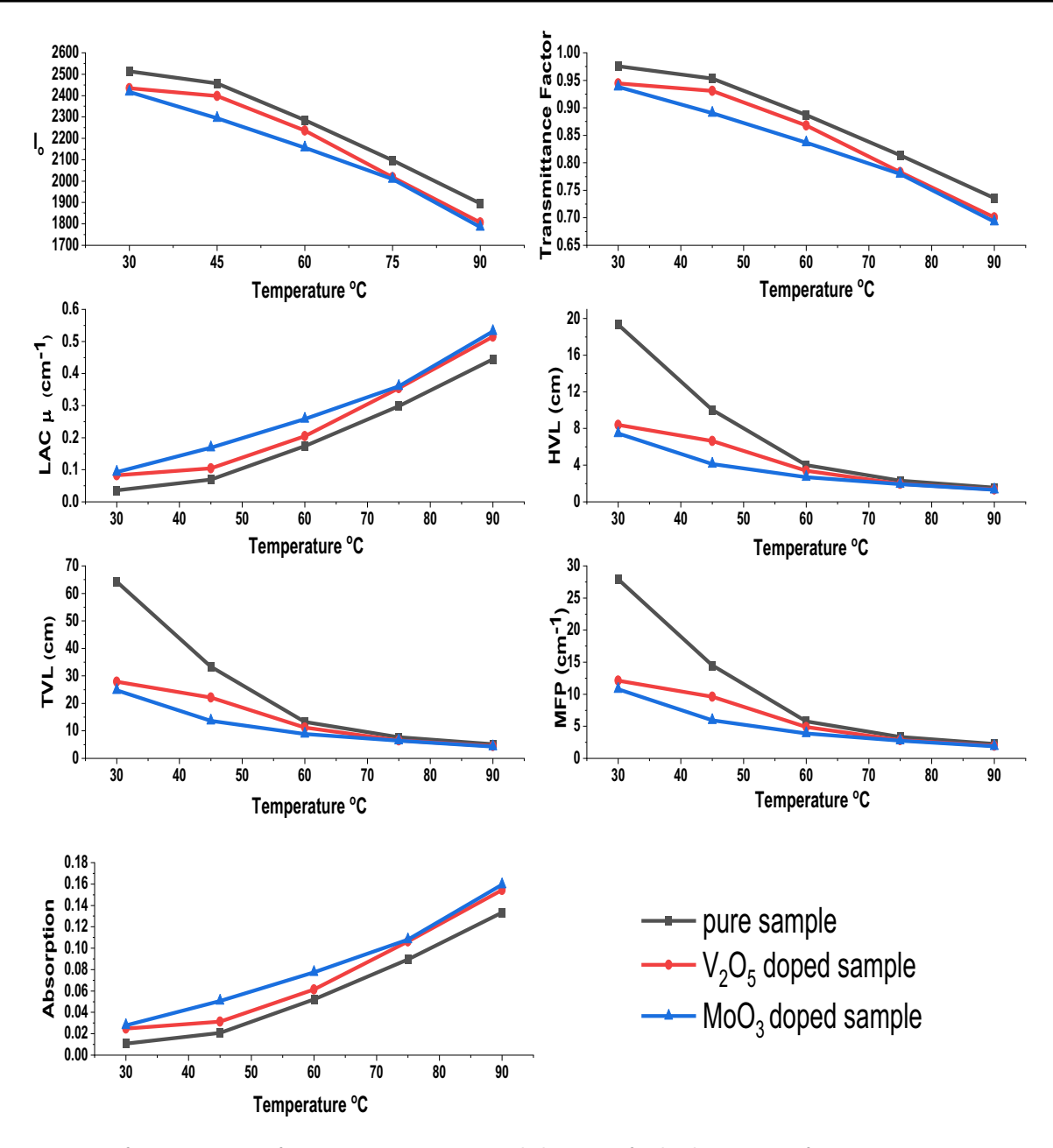


Fig. 5 Comparison of Io, transmittance factor, LAC, HVL, TVL, MFP and Absorption for the three variants for source Cs-137

the samples tested, the molybdenum-doped liquid exhibited the highest LAC, outperforming both vanadium-doped and pure liquids. This indicates that higher temperatures enhance the radiation shielding capability. The evaluation of the LAC ( $\mu$ ) was conducted using Beer-Lambert's law, demonstrating that increased temperature contributes to improved radiation shielding performance,

$$I = I_0 \exp(-\mu x) \tag{1}$$

$$\mu = \ln(I_0/I) / x \tag{2}$$

where, I is the attenuated radiation intensity after travelling through the sample medium by thickness x, and  $\mu$  is the linear attenuation coefficient.

Further the effects of the shielding gamma rays by Half Value Layer (HVL) and Tenth Value Layer (TVL) were also reported. The thickness with which the absorber reduces the gamma radiation by half and one tenth were said to be



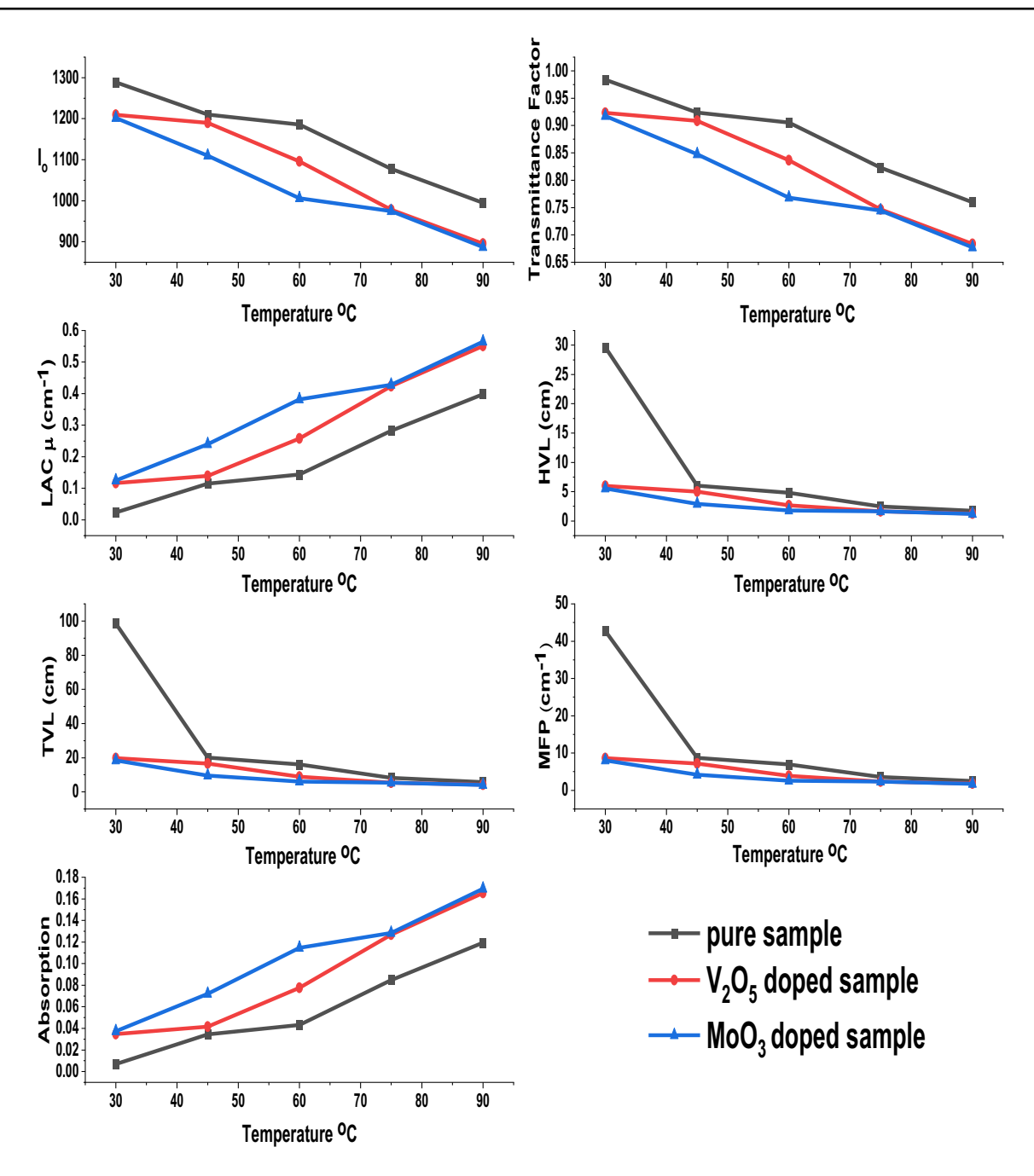


Fig. 6 Comparison of Io, transmittance factor, LAC, HVL, TVL, MFP and Absorption for the three variants for source Na-22

HVL and TVL, respectively. The HVL and TVL values are obtained from the Eqs. 4 and 5, respectively [43, 44]. The mean distance with which two consecutive photons interact is the Mean Free Path (MPF) and is obtained using Eq. 6. Likewise, the absorption factor was obtained from the Eq. 7.

$$Transmission factor = I/I_0$$
 (3)

Half Value Layer, 
$$HVL = X_{1/2} = \ln 2/\mu$$
 (4)

Tenth Value Layer, 
$$TVL = X_{1/10} = \ln 10/\mu$$
 (5)



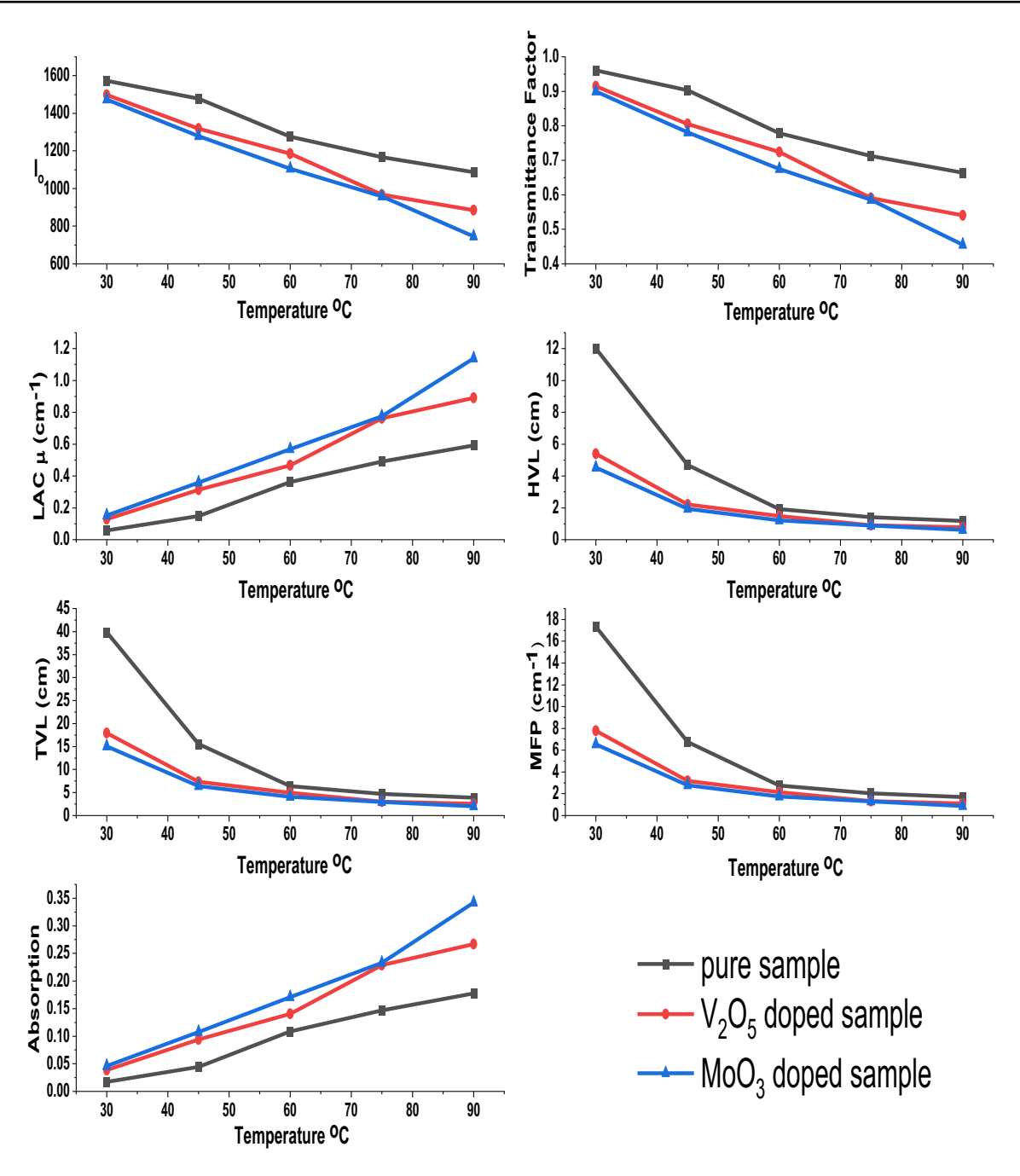


Fig. 7 Comparison of Io, transmittance factor, LAC, HVL, TVL, MFP and Absorption for the three variants for source Co-60

Mean Free Path, MFP = 
$$\mu$$
 (6)

Absorption factor 
$$= -I/I_O$$
 (7)

The experiment was successfully conducted and the transmitted intensity, linear attenuation co-efficient, transmission factor, absorption, half value layer, tenth value layer, mean free path were reported for each sample for each source. Table 1, 2, 3 provides the data of shielding properties of pure sample, vanadium and molybdenum doped IFF samples for Cs-137 source. Similarly, Tables 4, 5, 6 provides the data against Na-22 source. Tables 7, 8, 9 for Co-60 and Tables 10, 11, 12, 13 for Ba-133 sources, respectively.



(2025) 7:926

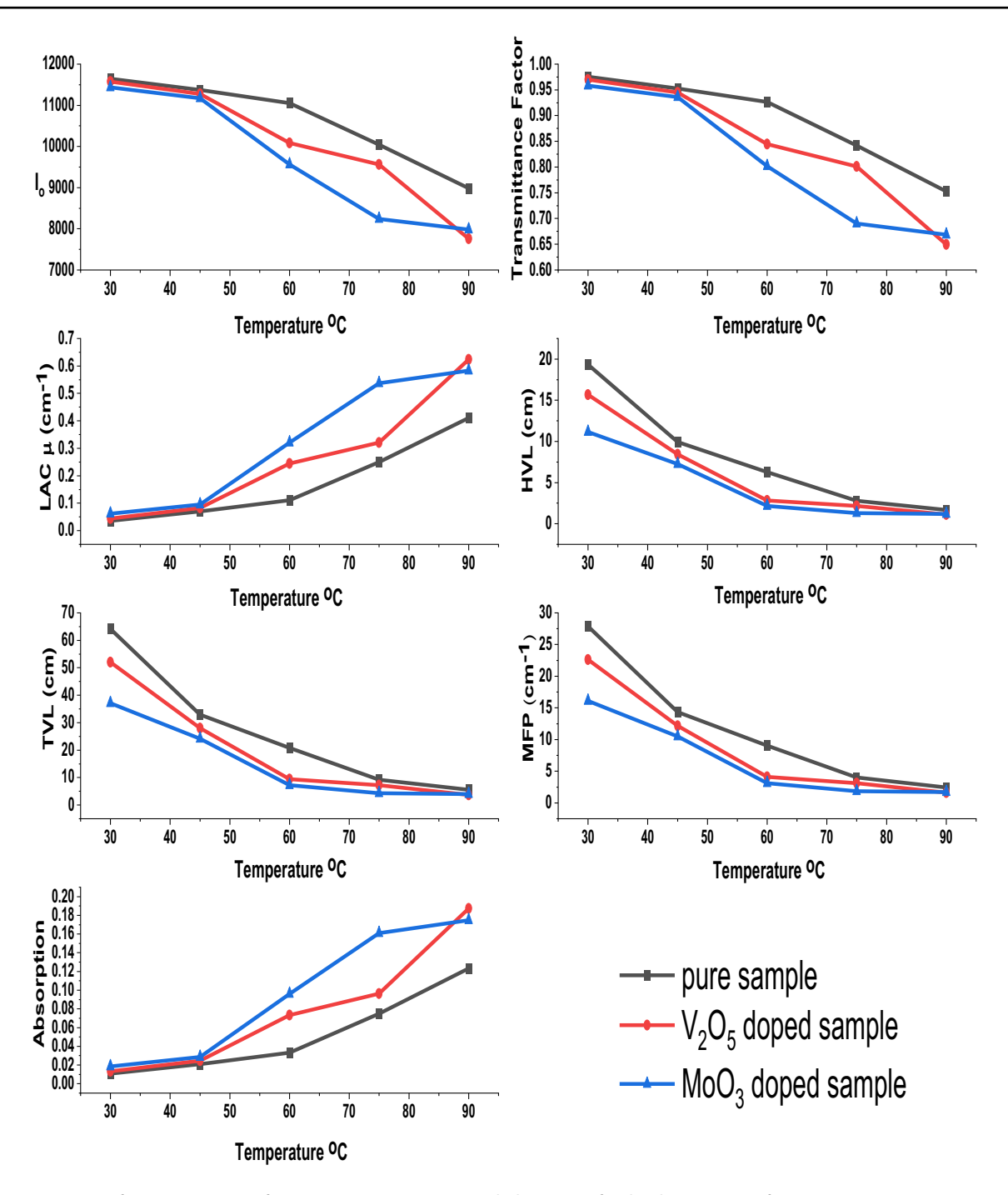


Fig. 8 Comparison of Io, transmittance factor, LAC, HVL, TVL, MFP and Absorption for the three variants for source Ba-133

The radiation attenuation parameters, that is, HVL, TVL and MFP increases with increase in temperature. As shown in the Figs. 5, 6, 7, 8, the transmitted intensity, transmittance factor, LAC, HVL, TVL, MFP and absorption factor were plotted for various gamma radiation emitting sources like Cs-137, Na-22, Co-60 and Ba-133. The transmitted intensity, transmittance factor, TVL, HVL and MFP decreases as the temperature increases. The variation trend of LAC and absorption factor are also plotted, with which it increases as the temperature of the samples were increased. Comparing all the three variants (pure, vanadium and molybdenum doped IFF samples) molybdenum doped IFF sample has the maximum values LAC and absorption factor and least transmitted intensity, transmittance factor, TVL, HVL and MFP.



Furthermore, the samples show observable variation in the radiation counts which in turn affects the absorption co efficient, LAC and MFP. For vanadium and molybdenum doped samples for Cs-137 source, the absorption factors are 0.1543 and 0.1594, LAC are 0.5146 cm<sup>-1</sup> and 0.5315 cm<sup>-1</sup> and MFP was 1.943 cm<sup>-1</sup> and 1.8811 cm<sup>-1</sup>. For Na-22 source the absorption factors are 0.1654 and 0.1693, LAC are 0.5514 cm<sup>-1</sup> and 0.5644 cm<sup>-1</sup> and MFP was 1.8132 cm<sup>-1</sup> and  $1.7715 \, \mathrm{cm}^{-1}$ . For Ba-133 source the absorption factors are 0.1871 and 0.1747, LAC are 0.6239  $\mathrm{cm}^{-1}$  and 0.5825  $\mathrm{cm}^{-1}$ and MFP was 1.6026 cm<sup>-1</sup> and 1.7165 cm<sup>-1</sup>. Here the reduction of all these factors could be observed but the difference seen is little. But for the Co-60 source the difference between these factors the absorption factors are 0.2671 and 0.3418, LAC are  $0.8903 \text{ cm}^{-1}$  and  $1.1396 \text{ cm}^{-1}$  and MFP was  $1.1231 \text{ cm}^{-1}$  and  $0.8774 \text{ cm}^{-1}$  from vanadium and molybdenum doped samples are evidently more. Since, these are liquid samples, even a small variation in the factors should be accounted. Herein, these two doped samples have a better performance for the Co-60 source compared to all the other sources. Additionally, within these two doped samples the molybdenum doped sample has exhibited performance compared to the other. This is solely because of the density variation between the molybdenum trioxide and vanadium pentoxide. The densities of the elements molybdenum and vanadium are  $\sim 10.22 \text{ g/cm}^3$  and  $\sim 6.11 \text{ g/cm}^3$ cm<sup>3</sup>. When considered as its oxides, the densities of molybdenum trioxide and vanadium pentoxide are ~ 4.69 g/ cm<sup>3</sup> and ~ 3.36 g/cm<sup>3</sup>. This becomes the major reason which affects the gamma photons transmission through the liquids. When the density increases the refractive index also increases, thus better IFF and shielding performance was obtained from molybdenum doped sample.

Moreover, addition of excess amount of metal part results in no IFF property. Thus, the heated solution never attains its liquid phase when the temperature is reduced. In short, this will be deleterious for the memory effect of the IFF. In summary, liquid radiation shielding represents a novel and promising approach to radiation protection, combining adaptability and advanced material science to address diverse needs across various domains.

# 4 Conclusion

The synthetic fluid combinations in the emerging scientific field of "inverse freezing fluids" which liquify at lower temperatures and freeze at higher temperatures. These types of new disciplines are still in the realm of fundamental sciences, where their practical applications have not yet been investigated and discovered. Ongoing research aims to optimize these properties to improve performance and safety. Emerging developments in this field suggest that liquid radiation shields could play a crucial role in future radiation protection technologies, offering a flexible and effective solution to a range of radiation-related challenges. This work is the first to provide a thorough explanation of the applications of inverse freezing fluids. In this case, we have chosen to investigate the gamma radiation shielding of the synthesised inverse freezing fluids, specifically for the pure, vanadium-doped, and molybdenum-doped samples. It is clear from the data presented and analysis that liquid mixtures, in particular inverse freezing fluids, can be utilized to shield against gamma radiation at different temperatures. The shielding properties improve with increasing temperature. Temperature has an impact on how much radiation may be absorbed and transmitted through the samples. Plots of transmitted intensity, transmittance factor, LAC, HVL, TVL, MFP and absorption for all the three variants are provided for better comparison to know how the molybdenum doped sample exhibits superior shielding compared to the other two synthesised samples. The Co-60 source the absorption factor is 0.3418, LAC is  $1.1396 \, \mathrm{cm}^{-1}$  and MFP was  $0.8774 \, \mathrm{cm}^{-1}$  for molybdenum doped samples which are evidently more compared to the vanadium doped samples. In conclusion, this is a novel and relevant approach, particularly for complex geometric structures where solid shielding becomes impractical in the area of gamma radiation shielding.

Acknowledgements We would like to express our gratitude to The National College, Jayanagar, Bangalore, India for providing the gamma ray spectrometer for this research work.

Author contributions Reshma Karunakaran—formal analysis, investigation, resources, data curation, writing-original draft, visualization. Rajagopal Shanmugasundaram—conceptualization, methodology, software, validation, formal analysis, investigation, resources, data curation, writing-original draft, visualization.

Data availability Data cannot be shared openly but are available on request from author.

## **Declarations**

Ethics approval and consent to participate Not applicable.



Competing interests The authors declare no competing interests.

Open Access This article is licensed under a Creative Commons Attribution-NonCommercial-NoDerivatives 4.0 International License, which permits any non-commercial use, sharing, distribution and reproduction in any medium or format, as long as you give appropriate credit to the original author(s) and the source, provide a link to the Creative Commons licence, and indicate if you modified the licensed material. You do not have permission under this licence to share adapted material derived from this article or parts of it. The images or other third party material in this article are included in the article's Creative Commons licence, unless indicated otherwise in a credit line to the material. If material is not included in the article's Creative Commons licence and your intended use is not permitted by statutory regulation or exceeds the permitted use, you will need to obtain permission directly from the copyright holder. To view a copy of this licence, visit http://creativecommons.org/licenses/by-nc-nd/4.0/.

# References

- Thomas GA, Symonds P. Radiation exposure and health effects—is it time to reassess the real consequences? Clin Oncol. 2016;28:231–6. https://doi.org/10.1016/j.clon.2016.01.007.
- 2. Deng Y, Liu J. Liquid metal based stretchable radiation-shielding film. J Med Devices Trans ASME. 2015. https://doi.org/10.1115/1.4029317.
- 3. Bakshi J. Radiation attenuation and stability of ClearView radiation shielding TM-A transparent liquid high radiation shield, 2018. www. health-physics.com.
- 4. Fuks L, Herdzik-koniecko I, Kiegiel K, Miskiewicz A, Zakrzewska-koltuniewicz G. Methods of thermal treatment of radioactive waste. Energies (Basel). 2022. https://doi.org/10.3390/en15010375.
- Osmanlioglu AE. Decontamination of radioactive wastewater by two-staged chemical precipitation. Nucl Eng Technol. 2018;50:886–9. https://doi.org/10.1016/j.net.2018.04.009.
- 6. Manos MJ, Kanatzidis MG. Metal sulfide ion exchangers: superior sorbents for the capture of toxic and nuclear waste-related metal ions. Chem Sci. 2016;7:4804–24. https://doi.org/10.1039/c6sc01039c.
- 7. Alwaeli M, Mannheim V. Investigation into the current state of nuclear energy and nuclear waste management—a state-of-the-art review. Energies (Basel). 2022. https://doi.org/10.3390/en15124275.
- 8. Ipek U, Öbek E, Akca L, Arslan El, Hasar H, Doğru M, Baykara O. Determination of degradation of radioactivity and its kinetics in aerobic composting. Bioresour Technol. 2002;84:283–6. https://doi.org/10.1016/S0960-8524(02)00024-X.
- 9. McCaffrey JP, Shen H, Downton B, Mainegra-Hing E. Radiation attenuation by lead and nonlead materials used in radiation shielding garments. Med Phys. 2007;34:530–7. https://doi.org/10.1118/1.2426404.
- Leszczyńska A, Njuguna J, Pielichowski K, Banerjee JR. Polymer/montmorillonite nanocomposites with improved thermal properties. Part I. Factors influencing thermal stability and mechanisms of thermal stability improvement. Thermochim Acta. 2007;453:75–96. https://doi.org/10.1016/j.tca.2006.11.002.
- 11. Horike S, Nagarkar SS, Ogawa T, Kitagawa S. A new dimension for coordination polymers and metal-organic frameworks: towards functional glasses and liquids. Angew Chem Int Ed. 2020;59:6652–64. https://doi.org/10.1002/anie.201911384.
- 12. Almuqrin A, Tijani SA, Al-Ghamdi A, Alhuzaymi T, Alotiby MF. Radiation shielding properties of high-density polyethylene (C2H4)/molybdenum III oxide (MoO3) polymer composites for dental diagnostic applications. J Radiat Res Appl Sci. 2023;16: 100681. https://doi.org/10.1016/j.jrras.2023.100681.
- 13. Muradov M, Baghirov MB, Eyvazova G, Gahramanli L, Mammadyarova S, Aliyeva G, Huseynov E, Abdullayev M. Influence of gamma radiation on structure, morphology, and optical properties of GO and GO/PVA nanocomposite. Radiat Phys Chem. 2023. https://doi.org/10.1016/j.radphyschem.2023.110926.
- 14. Abualroos NJ, Yaacob KA, Zainon R. Radiation attenuation effectiveness of polymer-based radiation shielding materials for gamma radiation. Radiat Phys Chem. 2023. https://doi.org/10.1016/j.radphyschem.2023.111070.
- 15. Ihsani RN, Gareso PL, Tahir D. An overview of gamma radiation shielding: enhancements through polymer-lead (Pb) composite materials. Radiat Phys Chem. 2024. https://doi.org/10.1016/j.radphyschem.2024.111619.
- Baghirov MB, Muradov M, Eyvazova G, Mammadyarova S, Gahramanli L, Aliyeva G, Huseynov E, Abdullayev M. Features of structure and optical properties GO and a GO/PVA composite subjected to gamma irradiation. RSC Adv. 2023;13:35648–58. https://doi.org/10.1039/ d3ra07186c.
- 17. More CV, Alsayed Z, Badawi MS, Thabet AA, Pawar PP. Polymeric composite materials for radiation shielding: a review. Environ Chem Lett. 2021;19:2057–90. https://doi.org/10.1007/s10311-021-01189-9.
- Singh VP, Badiger NM, Kothan S, Kaewjaeng S, Korkut T, Kim HJ, Kaewkhao J. Gamma-ray and neutron shielding efficiency of Pb-free gadolinium-based glasses. Nucl Sci Tech. 2016. https://doi.org/10.1007/s41365-016-0099-1.
- 19. Huseynov EM. FTIR spectroscopy of ZrC nanoparticles under the gamma radiation. Spectrochim Acta A Mol Biomol Spectrosc. 2023. https://doi.org/10.1016/j.saa.2022.122032.
- 20. Huseynov EM, Hakhiyeva RR, Mehdiyev NM. FTIR study of nanocrystalline titanium carbide (TiC) particles exposed to gamma radiation. Solid State Commun. 2024. https://doi.org/10.1016/j.ssc.2023.115417.
- 21. Huseynov E, Garibov A, Mehdiyeva R, Huseynova E. Fourier transform infrared spectroscopic study of gamma irradiated SiO2 nanoparticles. Int J Mod Phys B. 2018. https://doi.org/10.1142/S0217979218500741.
- 22. Hakhiyeva RR, Abiyev AS, Huseynov EM. Comprehensive analysis of gamma irradiation-induced crystallographic transformations in TiC nanoparticles using X-ray diffraction techniques. Radiat Phys Chem. 2025. https://doi.org/10.1016/j.radphyschem.2024.112363.
- 23. Huseynov EM, Hakhiyeva RR. Investigation of gamma irradiated nanocrystalline titanium carbide particles using thermal methods. J Radioanal Nucl Chem. 2023;332:3779–85. https://doi.org/10.1007/s10967-023-09077-y.



- 24. Nikbin IM, Rafiee A, Dezhampanah S, Mehdipour S, Mohebbi R, Moghadam HH, Sadrmomtazi A. Effect of high temperature on the radiation shielding properties of cementitious composites containing nano- Bi2O3. J Market Res. 2020;9:11135–53. https://doi.org/10.1016/j.imrt.2020.08.018.
- 25. Kim J, Seo D, Lee BC, Seo YS, Miller WH. Nano-W dispersed gamma radiation shielding materials. Adv Eng Mater. 2014;16:1083–9. https://doi.org/10.1002/adem.201400127.
- 26. Huseynov EM, Atakishiyeva JG. Characterizing neutron irradiation-induced effects in the nanocrystalline B4C particles using EPR spectroscopy. Solid State Sci. 2024. https://doi.org/10.1016/j.solidstatesciences.2024.107604.
- 27. Huseynov EM, Jazbec A. Application of neutron transmutation technology to control the physical properties of nanoparticles at the atomic scale. Carbon N Y. 2024. https://doi.org/10.1016/j.carbon.2024.119568.
- 28. Huseynov EM, Huseynova EA, Jazbec A. EPR spectroscopic characterization of neutron-irradiated nanocrystalline anatase particles. Physica B Condens Matter. 2025. https://doi.org/10.1016/j.physb.2024.416786.
- 29. Huseynov E, Jazbec A, Snoj L. Temperature vs. impedance dependencies of neutron-irradiated nanocrystalline silicon carbide (3C-SiC). Appl Phys A Mater Sci Process. 2019. https://doi.org/10.1007/s00339-018-2294-x.
- 30. Huseynov EM, Garibov AA, Valiyev SP. EPR study of silicon nitride (Si3N4) nanoparticles exposed to neutron irradiation. Radiat Phys Chem. 2022. https://doi.org/10.1016/j.radphyschem.2022.110087.
- 31. Huseynov EM, Huseynova EA. Infrared spectroscopy of nanocrystalline anatase (TiO2) particles under the neutron irradiation. Opt Mater (Amst). 2023. https://doi.org/10.1016/j.optmat.2023.114351.
- 32. Huseynov EM, Naghiyev TG. Low temperature DSC investigation of neutron irradiated non-crystalline Si3N4 nanoparticles. J Non Cryst Solids. 2025. https://doi.org/10.1016/j.jnoncrysol.2024.123272.
- 33. Karunakaran R, Shanmugasundaram R. Insight into unusual complex thermodynamical behaviour of citric acid and ethanolamine solution. Discov Mater. 2025;5:18. https://doi.org/10.1007/s43939-025-00192-z.
- 34. El-Khatib AM, Badawi MS, Thabet AA, Jovanovic SI, Gouda MM, Mohamed MM, Dlabac AD, Abd-Elzaher M, Mihaljevic NN, Abbas MI. Well-type Nal(Tl) detector efficiency using analytical technique and ANGLE 4 software based on radioactive point sources located out the well cavity. Chin J Phys. 2016;54:338–46. https://doi.org/10.1016/j.cjph.2016.03.019.
- 35. Badawi MS, Gouda MM, Nafee SS, El-Khatib AM, El-Mallah EA. New algorithm for studying the effect of self attenuation factor on the efficiency of γ-rays detectors. Nucl Instrum Methods Phys Res A. 2012;696:164–70. https://doi.org/10.1016/j.nima.2012.08.089.
- 36. El-Khatib AM, Gouda MM, Badawi MS, Nafee SS, El-Mallah EA. Newanalytical approach to calibrate the Nal (TI) detectors using spherical radioactive sources. Radiat Prot Dosimetry. 2013;156:109–17. https://doi.org/10.1093/rpd/nct048.
- 37. Laguerie C, Aubry M, Couderc J-P. Some physicochemical data on monohydrate citric acid solutions in water: solubility, density, viscosity, diffusivity, pH of standard solution, and refractive index. J Chem Eng Data. 1976;21:85–7.
- 38. Deshmukh SD, Pattebahadur KL, Undre PB, Khirade SS. Study of refractive index, density and their excess properties of binary mixture. Bionano Front. 2015;8(3):223.
- 39. Chiang D, Chiu PK, Hsiao WT, Tseng SF. Determination of the refractive index of molybdenum using a spectrophotometric method. Sens Mater. 2019;31:3517–26. https://doi.org/10.18494/SAM.2019.2500.
- 40. Jagannath G, Pramod AG, Keshavamurthy K, Swetha BN, Eraiah B, Rajaramakrishna R, Ramesh P, Prashantha SC, Abdullah MS, Sayyed MI. Nonlinear optical, optical limiting and radiation shielding features of Eu3+ activated borate glasses. Optik (Stuttg). 2021. https://doi.org/10.1016/j.ijleo.2021.166563.
- 41. Al-Hadeethi Y, Sayyed MI, Kaewkhao J, Askin A, Raffah BM, Mkawi EM, Rajaramakrishna R. Physical, structural, optical, and radiation shielding properties of B2O3–Gd2O3–Y2O3 glass system. Appl Phys A Mater Sci Process. 2019. https://doi.org/10.1007/s00339-019-3115-6.
- 42. Kaewjaeng S, Wantana N, Kothan S, Rajaramakrishna R, Kim HJ, Limsuwan P, Kaewkhao J. Effect of Gd2O3 on the radiation shielding, physical, optical and luminescence behaviors of Gd2O3–La2O3–ZnO–B2O3–Dy2O3 glasses. Radiat Phys Chem. 2021. https://doi.org/10.1016/j.radphyschem.2021.109500.
- 43. Al-Hadeethi Y, Sayyed MI, Kaewkhao J, Raffah BM, Almalki R, Rajaramakrishna R. An extensive investigation of physical, optical and radiation shielding properties for borate glasses modified with gadolinium oxide. Appl Phys A Mater Sci Process. 2019. https://doi.org/10.1007/s00339-019-3053-3.
- 44. Wang K, Hu J, Chen T, Tang J, Zhai Y, Feng Y, Zhao Z, Fan H, Wang K. Radiation shielding properties of flexible liquid metal-Galn alloy. Prog Nucl Energy. 2021. https://doi.org/10.1016/j.pnucene.2021.103696.

Publisher's Note Springer Nature remains neutral with regard to jurisdictional claims in published maps and institutional affiliations.

